metals

MDPI

Article

Estimation of Critical Dimensions for the Crack and Pitting Corrosion Defects in the Oil Storage Tank Using Finite Element Method and Taguchi Approach

Mostafa Omidi Bidgoli [1,*], Kazem Reza Kashyzadeh [2], Seyed Saeid Rahimian Koloor [3,*] and Michal Petru [3]

[1] Department of Mechanical Engineering, Islamic Azad University, Badroud Branch, Badroud 8764136545, Isfahan, Iran

[2] Department of Mechanical and Instrumental Engineering, Academy of Engineering, Peoples' Friendship University of Russia (RUDN University), Miklukho-Maklaya 6, 117198 Moscow, Russia; kazem.kashyzadeh@gmail.com

[3] Institute for Nanomaterials, Advanced Technologies and Innovation, Technical University of Liberec, Studentska 2, 461 17 Liberec, Czech Republic; michal.petru@tul.cz

* Correspondence:mostafaomidibidgoli@gmail.com (M.O.B.); s.s.r.koloor@gmail.com (S.S.R.K.); Tel.: +42-079-227-0479 (S.S.R.K.)

Received: 15 September 2020; Accepted: 9 October 2020; Published: 14 October 2020

Abstract: Tanks play an important role in storing crude oil. Therefore, the maintenance and service life of tanks are very important for oil companies. In this regard, knowledge on the state of the critical conditions of various existing defects, such as cracks and pitting corrosion defects, can play an essential role in providing a better service to these huge metal structures. In the present research, the basic theories relating to crack defects were discussed. Then, an oil reserve in one of the island states of the country was modeled and analyzed by considering different types of defects using Finite Element (FE) simulation. Next, the critical dimensions of cracks and corrosion holes were identified in a number of cases. Eventually, the Taguchi Approach (TA) was used to investigate the effect of different parameters related to the various defects, such as length, depth and diameter, on the maximum stress. The results indicated that the effect of the crack and pitting corrosion depth is superior to the effect of the length and diameter for defects of crack and pitting corrosion, respectively.

Keywords: critical size; crack; pitting corrosion; oil storage tank; FEM; Taguchi Approach

1. Introduction

Nowadays, reservoirs are widely used in various industries, especially in oil, gas and petrochemical companies, so that their exact and stable efficiency is important for storing different materials. In this case, crude oil storage tanks also need to be kept properly, which is important when it is possible to identify the situation and critical conditions of defects during the cyclic inspections.

Most important defects in these huge metal structures are cracks and pitting corrosions. The first attempts to solve the cracked cylinder problem were carried out by Androwood in 1972 [1]. Afterwards, in 1982, Rajo and Newman analyzed longitudinal cracks in pressure vessels using a 3-D finite element model [2]. In 1993, Carpinteri utilized finite element simulation to analyze the semi-elliptical cracks in metal bars under uniaxial loading [3]. Moreover, Carpinteri et al. reported similar results for the behavior of semi-elliptical cracks in tubes under a cyclic flexural moment [4]. Font et al. examined a circular rod with an elliptical sidewall crack [5,6]. In a participatory program in

Canada, several experiments were conducted to predict the failure behavior of a damaged pressure vessel [7]. Then, Carpinteri conducted research on the cracked tubes [8]. Following these activities, a number of high-pressure cylinders of aluminum and steel were tested under hydrostatic pressure by the center of USA's nondestructive testing analysis [9]. Shahani et al. calculated the stress intensity factor for a semi-elliptical crack in a thick-walled cylindrical tank under a bending moment using an FE analysis and experiment data [10,11]. Recently, a new technique was presented to predict the stress intensity factor of Mode-I for an elliptical crack in a tube [12]. Moreover, the stress intensity factor was calculated for a semi-elliptical crack in a hollow cylinder tank under combined loadings [13]. Petan and Kizingloo performed several tests to determine the explosion pressure and critical region in a vehicle's gas cylinders [14]. Furthermore, laboratory investigations were carried out on the critical region of the pressure vessels and were compared with analytical results [14]. Kasai et al. evaluated back-side flaws of the bottom plates on an oil storage tank [15]. Kim et al. carried out a failure analysis of fillet joint cracking in an oil storage tank [16]. Godoy obtained the buckling of fixed-roof aboveground oil storage tanks under heat induced by an external fire [17]. Yang et al. derived an analytical formula for the elastic-plastic instability of large oil storage tanks [18]. Kasai et al. predicted the maximum depth of corrosion in an oil storage tank using extreme value analysis and Bayesian inference [19]. Cheng et al. studied a stability parameter analysis of a composite foundation of an oil storage tank in a loess area treated with a compaction pile [20].

Because oil storage tanks are out of service due to corrosion and cracking defects, it is possible to prevent the failure and destruction caused by these defects by having information on critical dimensions. Therefore, in this research, the most important defects in one of the reservoirs with a capacity of 1,350,000 barrels were investigated and analyzed. The critical size of cracks and pitting corrosion were determined. The Taguchi approach and analysis were applied for the first time for the various defects of corrosion. The results obtained by analyzing the defects and identifying critical dimensions can be useful for improving the inspection and prevention of future events.

2. Types of Defects in the Oil Storage Tanks

The most important defects in the oil storage tanks are cracks and pitting corrosion. Generally, these defects are due to one of the following reasons:

1. Defects due to inaccuracy in the construction, implementation and assembling of the structure.
2. Defects that occur during the storage of oil and exploitation of reservoirs.

2.1. Pitting Corrosion

Corrosion effects in oil storage tanks are divided into both internal and external types. However, most of the corrosion occurs in the inner surface at the bottom of the oil storage tanks, which sometimes completely pierces the surface as an effect of the environmental condition. The pit is a highly localized corrosion that also causes metal holes. These holes may have different diameters, but in most cases their diameter is small. The pits are sometimes separated and sometimes close together to form a roughness surface. Pitting is one of the most destructive and worst types of corrosion. Because of perforation, the metals become unusable. However, the weight loss due to this corrosion is negligible [21]. Figure 1 shows the corrosion phenomenon at the bottom of an oil storage tank and a schematic of the crack in the tank with the geometric parameters studied in this research such as the length, angle and depth of crack.

Experts in the field of corrosion believe that the best coatings, when used along with the cathodic protection system, only reduce the corrosion by 70% and that it can never be reduced to zero [21]. Although corrosion cannot be completely eliminated, its effects can be minimized by applying new methods such as Cathodic protection, industrial coatings and so on.

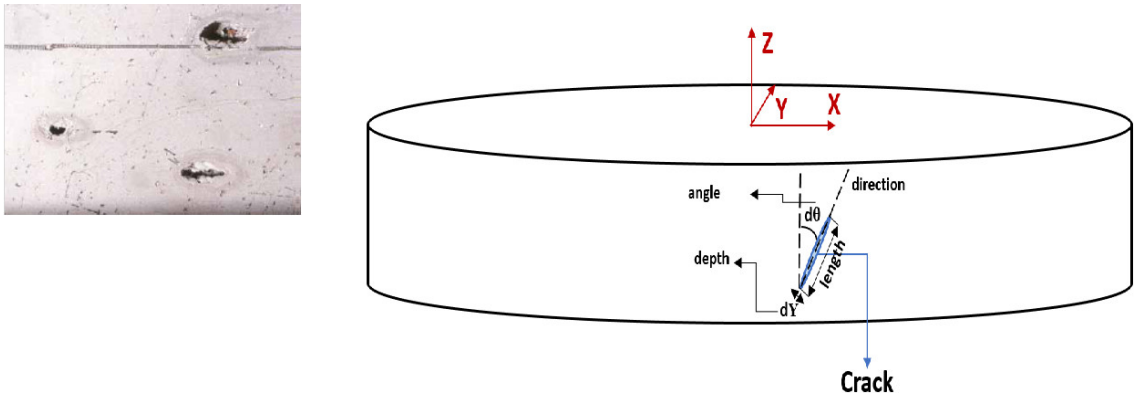

Figure 1. The defect of the pitting corrosion at the bottom of an oil storage tank and a schematic of the crack in the tank with the geometric parameters studied in this research such as the length (mm), angle (degree) and depth of the crack (mm).

2.2. Crack

Cracks are one of the defects to occur the most during the implementation and construction stages of a tank, and they have rarely been observed in oil storage tanks. However, the nature of these cracks is small, and they are most commonly found in the weld areas. Certainly, these cracks will grow and can damage the reservoir. In welding structures, a variety of arrangements is needed to prevent defects. Typically, the failure of pressure vessels during their service life will result in irreparable damage that not only causes economic losses. In the design process of pressure vessels, the issue of stress concentration inside the weld must be considered, especially for containers that have been kept in service for a long time [22]. In this research, if the crack angle is zero degrees (parallel to the height of the tank), it is called a longitudinal crack. Similarly, if the angle of the crack is 90 degrees to the height of the tank, it is a transverse crack. Finally, directional cracks are also called cracks, which in the present research were only examined at 45 degrees.

3. Finite Element Simulation

The geometric characteristics, material and thickness of sheets used in the tank are reported in Table 1, and the image of this tank is shown in Figure 2.

Table 1. Geometric characteristics of the oil storage tank.

Parameter	Value	Unit
Diameter	119.5	Meter
Height	19	Meter
Type of roof	Floating	
Floor	A283 Gr C, 7 mm	
Floor margin sheet	A537 Gr II, 20 mm	
First round sheet	A537 Gr I, 43 mm	
Second round sheet	A537 Gr I, 42 mm	
Third round sheet	A537 Gr I, 35 mm	
Fourth round sheet	A537 Gr I, 28 mm	
Fifth round sheet	A537 Gr I, 22 mm	
Sixth round sheet	A537 Gr I, 16 mm	
Seventh round sheet	A516 Gr 60, 13 mm	
Eighth sheet	A516 Gr 60, 11 mm	
Roof	A283 Gr C, 5 mm	

Figure 2. Image of the oil storage tank that was studied in this research.

The oil storage tank was modeled in FE software (ABAQUS, version 14.1, Dassault Systèmes Simulia Corp., Johnston, RI, USA) using an S4R element type as a shell body. The mesh convergence was investigated [23–25], and the final FEM was prepared with 30,000 elements (Figure 3).

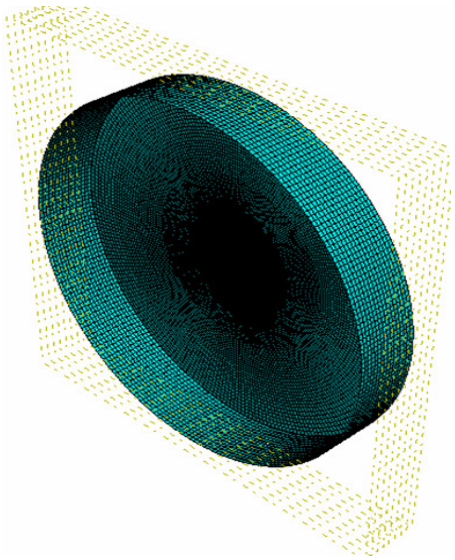

Figure 3. Finite element model of the oil tank.

The boundary conditions were considered as follows:

Around the tank floor:

$$U_1 = U_2 = U_3 = U_{R1} = U_{R2} = U_{R3} = 0 \quad (1)$$

The U_1, U_2, U_3 are linear displacement components, and U_{R1}, U_{R2}, U_{R3} are rotational displacement components around the coordinate axes.

The external surface of the tank floor:

$$U_3 = 0 \quad (2)$$

The oil storage tank without any defects was analyzed under hydrostatic pressure ($p = \rho g h =$ 160,295.4 Pa) to determine the critical region. After that, the effect of the defects was investigated, and the critical stress was obtained using two different methods (analytical and FEM).

In the hydrostatic pressure relationship, ρ, g, h are the fluid density, gravity acceleration and tank height, respectively.

3.1. Analytical Solution

The environmental and axial stresses in a cylinder are calculated in the following form [26]:

$$\sigma_h = \frac{P \times R}{B} \tag{3}$$

$$\sigma_a = \frac{P \times R}{2B} \tag{4}$$

where R and B are the radius and thickness of the tank, respectively. The environmental stress is the force that is applied peripherally (perpendicular to the axis and radius of the body) to the cylindrical wall. The tank wall is made up of eight different thickness sections with a constant height of 375 mm. Eventually, the maximum stress obtained was equal to 222.7 MPa.

3.2. FE Solution

The maximum stress was extracted from ABAQUS software. This value is 218.7 MPa, which has a good accuracy compared to the analytical result (222.7 MPa) with a 1.79% error. The contour of the equivalent von Mises stress is illustrated in Figure 4.

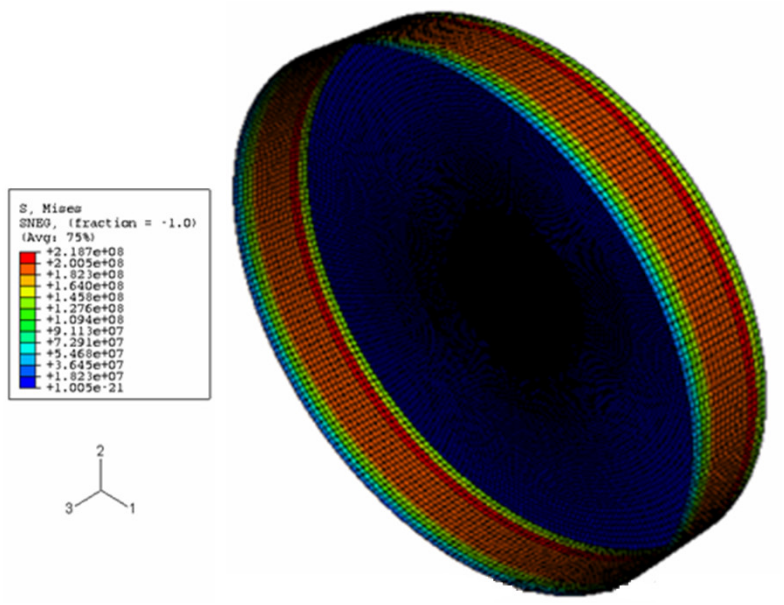

Figure 4. The von Mises stress contour of the oil storage tank under the hydrostatic pressure in MPa.

3.3. FE Model of Crack and Pitting Corrosion

There are various techniques to model crack and corrosion defects using FEM. One of these methods is the shell-to-solid coupling of elements, in which multipoint constraints are used, as demonstrated in Figure 5. In fact, the FE software provides continuity and integrity between the shell and solid elements by assigning special constraints [27,28].

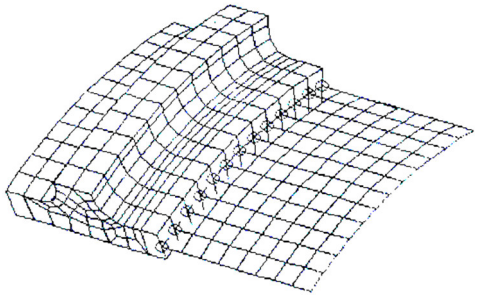

Figure 5. Schematic of the shell-to-solid coupling of elements.

First, a complete geometry was modeled using shell elements to validate this technique. Then, a new model with the same conditions was analyzed by utilizing a combination of shell and solid elements. The depth of the cavity and crack in the area was also modeled in the solid element so that the elements of the defect area were of a solid type and the areas without defects were modeled with the shell element. In this regard, a middle part of the shell was modeled as the volume. The contours of the von Mises stress for both models including only shell elements and combination of shell and solid elements are illustrated in Figure 6(a) and Figure 6(b), respectively.

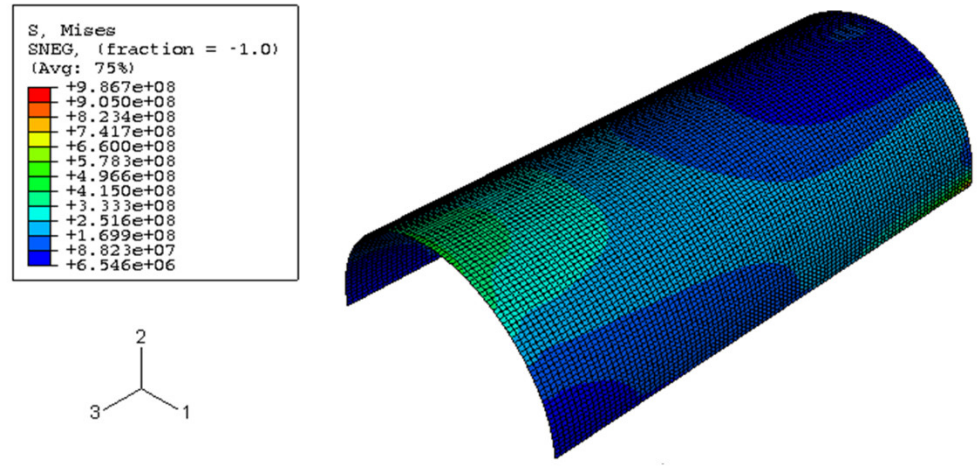

(**a**)

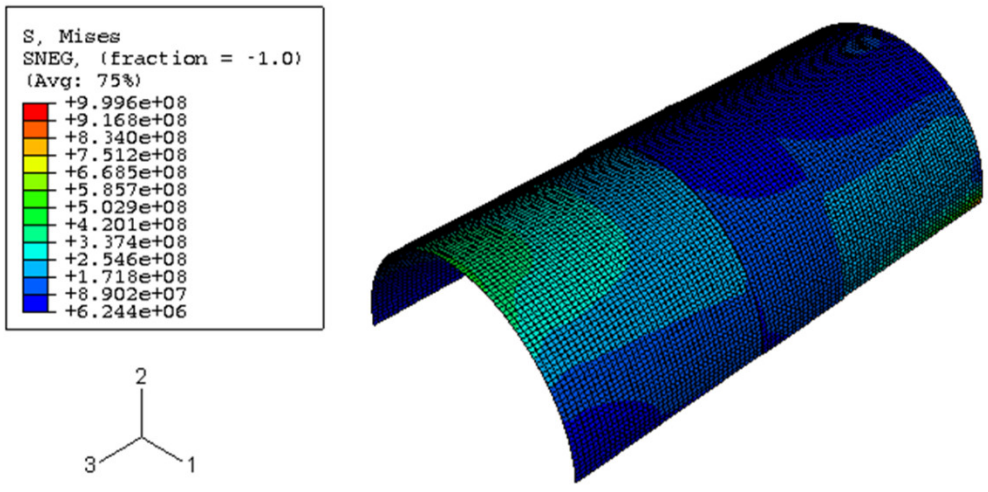

(**b**)

Figure 6. The contour of the equivalent von Mises stresses for both FE models: (**a**) Shell element only and (**b**) combination of shell and solid elements.

As shown in Figure 6, the difference between the results of various models (von Mises stress) is about 1.3%. However, the deformation is equal in the two models. In the finite element models, the stress level in the shell elements with the shell-to-solid elements is less than 10%. Therefore, this method can be used with a good accuracy for modeling and analyzing defects.

4. Taguchi Approach

Various Design of Experiments (DOE) techniques are used to reduce the number of experiments, cost, and time for studying the response behavior in terms of different variables. Meanwhile, the Taguchi algorithm proposes the minimum number of tests to evaluate the effects of input parameters [29–34]. In this strategy, a set of tables is set up as an orthogonal array. These arrays make it possible to obtain the main and interaction effects of different parameters by performing the least number of runs. In other words, this is the biggest advantage of the Taguchi method over other DOE techniques. In general, there are two models for analyzing results (standard and signal-to-noise ratio). The standard model depends on computing the impact of factors and on doing an analysis of variance. The subsequent model looks at the scattering close to a certain value. As the value of this ratio (signal/noise) increases, the scattering decreases, and in this case the effect of that parameter will be more important. Moreover, the Taguchi sensitivity analysis can also predict responses for other modes. Previous published papers show that the Taguchi prediction algorithm is very suitable for industrial components and has an acceptable accuracy [29,31,33,35]. Accordingly, the Taguchi method was used to determine the effect of different parameters of various defects, including cracks and pitting corrosion, on the critical equivalent stress of an oil storage tank. In the present research, two important defects, including a crack and pitting corrosion, were investigated in an oil storage tank. Defect geometry is one of the most important parameters affecting the behavior of structures under different loads and working conditions. Therefore, the aim of this paper was to obtain the critical value of the geometric parameters of both defects and also the effect of geometric parameters on the behavior of the structure. In the two-dimensional problems, the parameters of the crack length and crack angle are important for the crack defect, and the diameter is also important for the defect of pitting corrosion. But in three-dimensional problems, the depth of the defect plays an important role. Hence, in the present research, three (length, angle and depth) and two (diameter and depth) geometric parameters were considered as input variables of the Taguchi approach to the crack and pitting corrosion defects, respectively. As is clear from this article, this research was conducted on a real structure in the industry, and the values considered for each of the input variables of the Taguchi analysis were selected based on events occurring in reality. The variable parameters considered in the Taguchi algorithm for the pitting corrosion defect, along with their different levels, are reported in Table 2.

Table 2. Characteristics of the variable parameters considered in the Taguchi algorithm for the pitting corrosion defect.

Levels	Variables	
	Parameter I: Depth	**Parameter II: Length**
A	50	10
B	100	15
C	150	20

The Taguchi orthogonal matrices with the characteristics L8 (4^1 & 2^1) and L9(3^2) are used to form the Taguchi analysis for the crack and pitting corrosion defects, as shown in Table 3 and Table 4, respectively.

Table 3. The layout of the orthogonal matrix L8 (stress is in MPa).

Angle	Run No.	Inputs		Output
		Parameter I	Parameter II	Stress
Zero	1	A	A	415.00
	2	A	B	415.20
	3	B	A	416.96
	4	B	B	417.60
	5	C	A	417.20
	6	C	B	418.00
	7	D	A	418.50
	8	D	B	419.00
45	1	A	A	416.40
	2	A	B	416.58
	3	B	A	417.40
	4	B	B	417.80
	5	C	A	418.20
	6	C	B	418.40
	7	D	A	419.00
	8	D	B	419.20
90	1	A	A	409.00
	2	A	B	409.11
	3	B	A	410.97
	4	B	B	412.35
	5	C	A	411.78
	6	C	B	412.42
	7	D	A	417.10
	8	D	B	417.73

Table 4. The layout of the orthogonal matrix L9 (stress is in MPa).

Run No.	Inputs		Output
	Parameter I	Parameter II	Stress
1	A	A	415.13
2	A	B	417.41
3	A	C	419.63
4	B	A	415.61
5	B	B	419.70
6	B	C	421.83
7	C	A	416.44
8	C	B	418.55
9	C	C	436.9

5. Results and Discussion

5.1. Finite Element Results

To determine the critical sizes of oil storage tanks' defects, cracks and pits with different lengths, diameters and depths were analyzed. Critical states were identified by selecting the stress field close to the yield stress of the target area (416.66 MPa). Surface defects were modeled using C3D8R elements in the critical region. The stress diagrams are depicted in terms of depth for cracks and pitting corrosions in various situations (Figures 7 and 8).

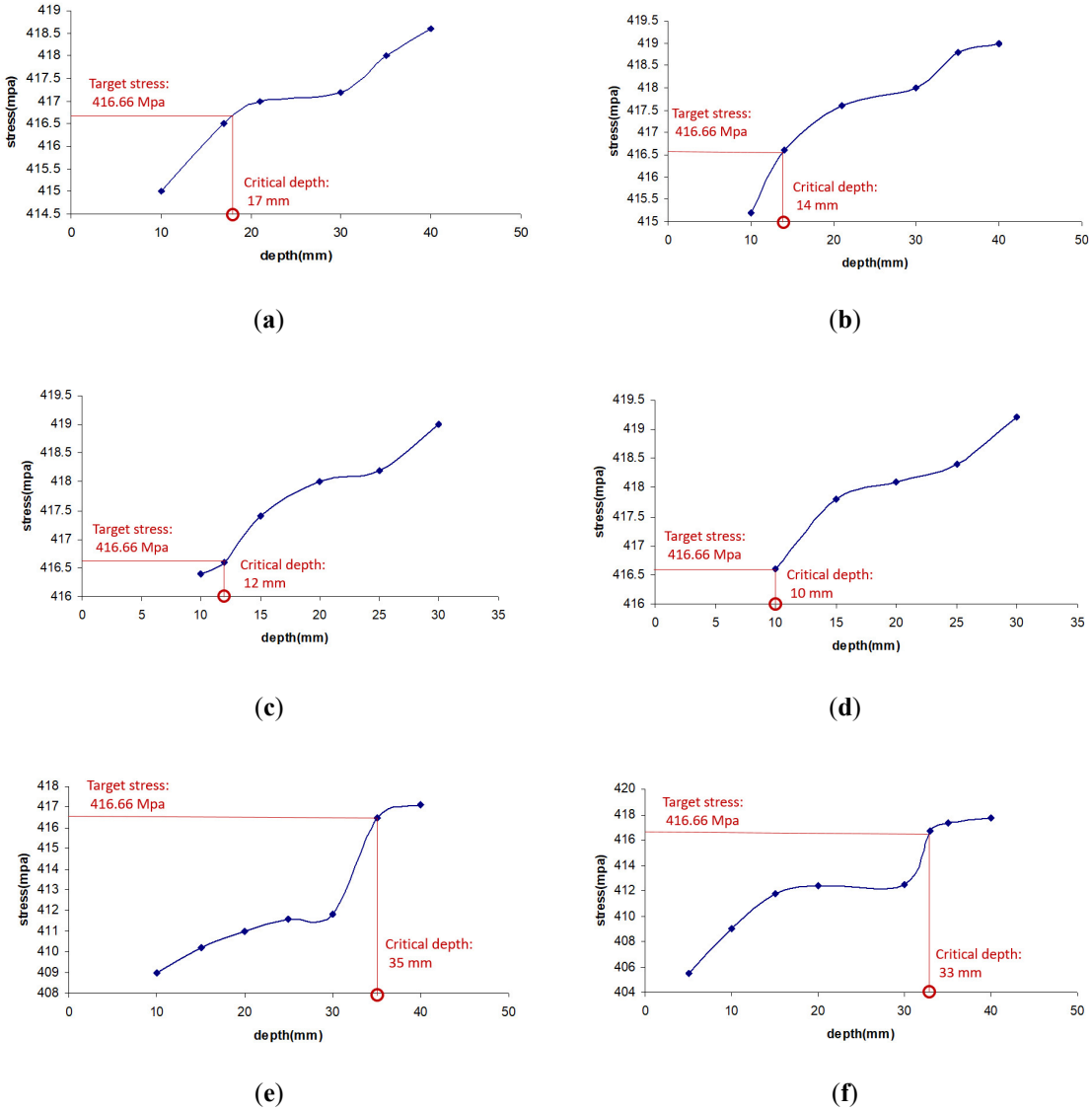

Figure 7. The stress diagram in terms of depth for cracks of various lengths and angles: (**a**) length = 300 and angle = 0; (**b**) length = 400 and angle = 0; (**c**) length = 150 and angle = 45; (**d**) length = 200 and angle = 45; (**e**) length = 300 and angle 90; (**f**) length = 400 and angle = 90.

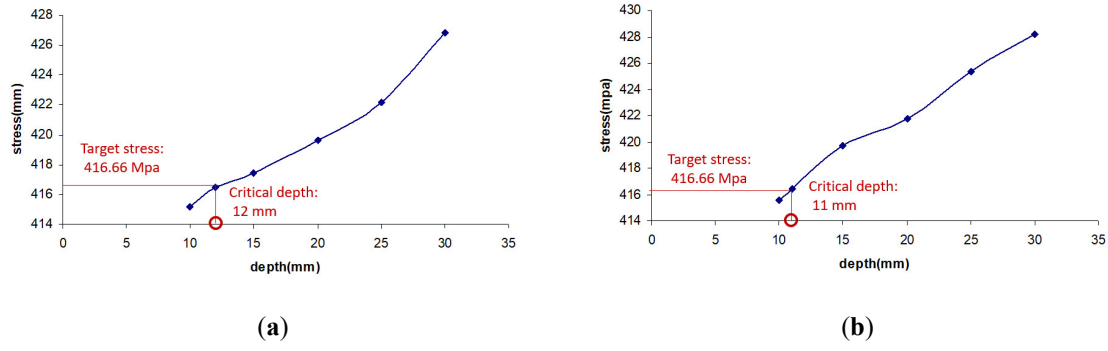

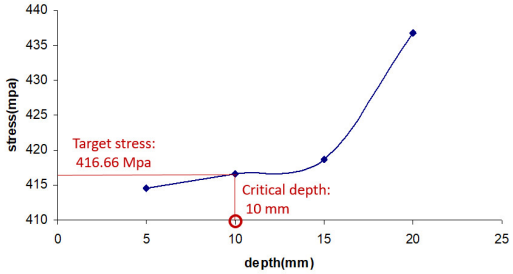

(**c**)

Figure 8. The stress diagrams in terms of depth for pitting corrosions with various diameters: (**a**) diameter = 50 mm; (**b**) diameter = 100 mm; (**c**) diameter = 150 mm.

From the FE results, the critical dimensions of the crack and the pitting corrosion defect are calculated and reported in Table 5 and Table 6, respectively.

Table 5. The critical sizes obtained from the FE analysis for the crack defect.

Crack Type	Critical Dimensions		
	Length (mm)	Depth (mm)	Angle
Environmental crack	300	17	0
Environmental crack	400	14	0
Crack	150	12	45
Crack	200	10	45
Longitudinal crack	300	35	90
Longitudinal crack	400	33	90

Table 6. The critical sizes obtained from the FE analysis for the pitting corrosion defect.

Defect Type	Critical Sizes	
	Diameter (mm)	Depth (mm)
Corrosion cavity	50	12
Corrosion cavity	100	11
Corrosion cavity	150	10

5.2. Taguchi Results

The most effective and least effective parameters based on Taguchi's analysis, along with the percentage of each parameter, were determined. Given the need to reduce the equivalent von Mises stress at the critical region of the oil storage tank, a smaller term is best used for the data analysis, in accordance with the following formula [35]:

$$\frac{S}{N} = -10Log[\frac{1}{n}(y_1^2 + y_2^2 + \cdots + y_n^2)] \quad (5)$$

where $y_1, y_2, \ldots, y_n$ represent the measured bent angles in the bending process, and each bending condition is repeated n times. Subsequently, the main influences of the S/N ratios and mean ratios at every parameter level were analyzed and plotted in Figures 9 and 10 for crack and pitting corrosion defects, respectively.

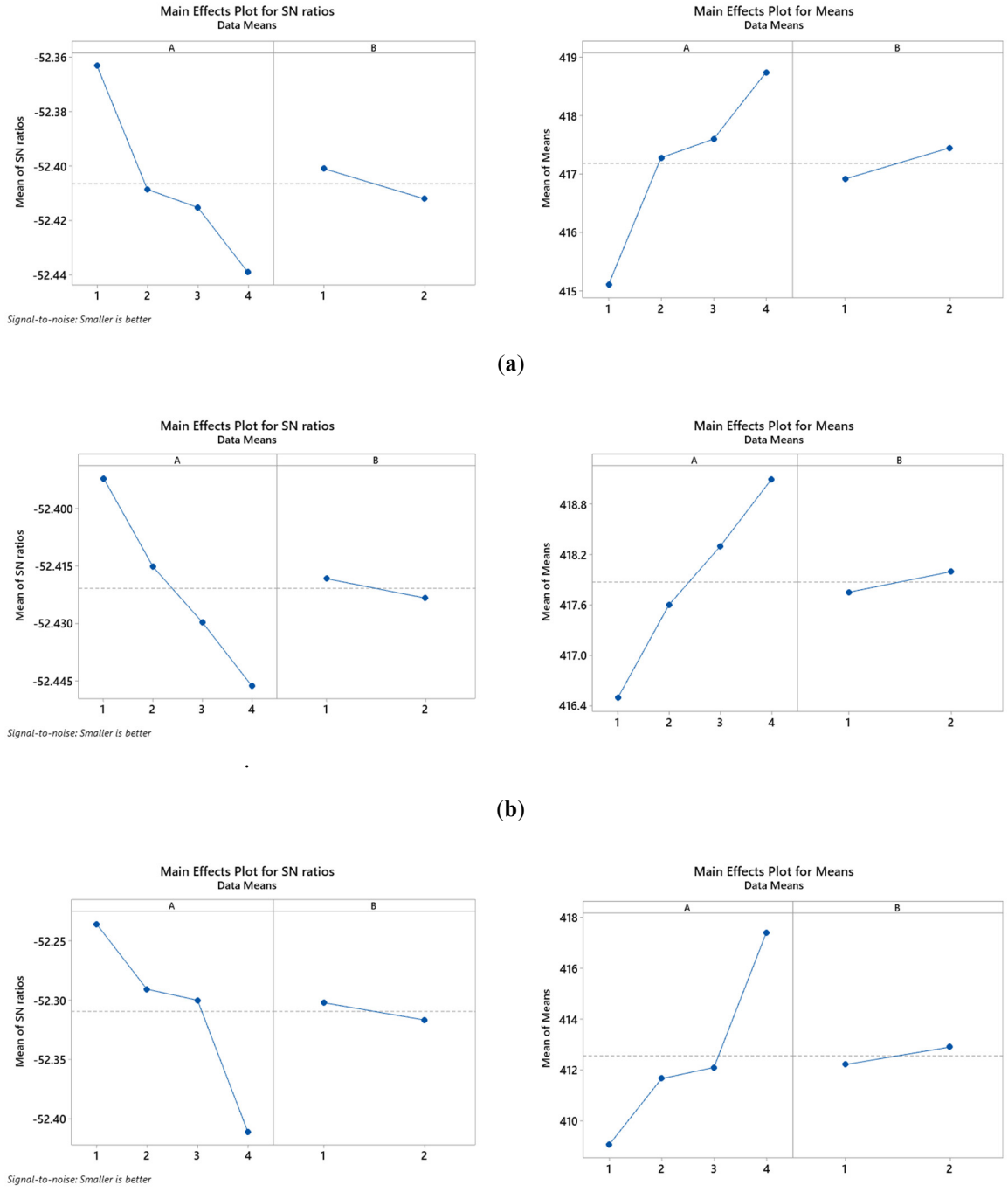

Figure 9. Influences of the S/N and mean ratios of all parameters related to the crack defect with different angles: (**a**) zero, (**b**) 45 and (**c**) 90.

As shown in Figures 9 and 10, the run number is sufficient to perform advisement regarding the Taguchi analysis because the diagram pattern of the S/N ratios is reversed when compared with the diagram pattern of the mean ratios [31–33]. In other words, the maximum situation in the diagram of the S/N ratio is the minimum value in the diagram of the mean ratio. From Figure 9, it is clear that increasing both the crack length and depth parameters leads to an increase in the stress of the structure and reduces its life. This result was also predictable, which indicates the correctness of the analysis. The results also show that increasing the crack angle from zero to 90 degrees reduces stress. In other words, it turns out that longitudinal cracking is the most destructive mode of cracking in a reservoir. In addition, failure Mode-I is predominant in this structure.

Figure 10 shows that the stress in the reservoir rises with increasing geometric parameters of pitting corrosion including the diameter and depth. However, it is not clear which of the geometric parameters is more effective.

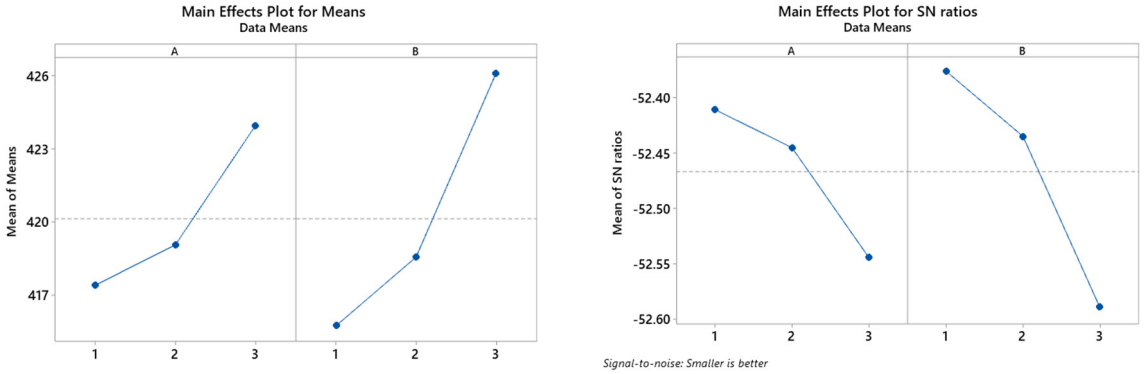

Figure 10. Influences of the S/N and mean ratios of all parameters related to the pitting corrosion defect.

Next, the effect of different parameters of the crack on the maximum von Mises stress is demonstrated in Figure 11(a). It is clear that the effect of the crack depth increases by raising the crack angle. Additionally, the effect of the crack length decreases by raising the angle of the crack. Eventually, the Taguchi sensitivity analysis was performed, and the result is demonstrated in Figure 11, which shows the most effective parameter for both defects. In addition, the least effective parameter is also specified. Moreover, the impact of different parameters of the pitting corrosion defect is displayed in Figure 11(b).

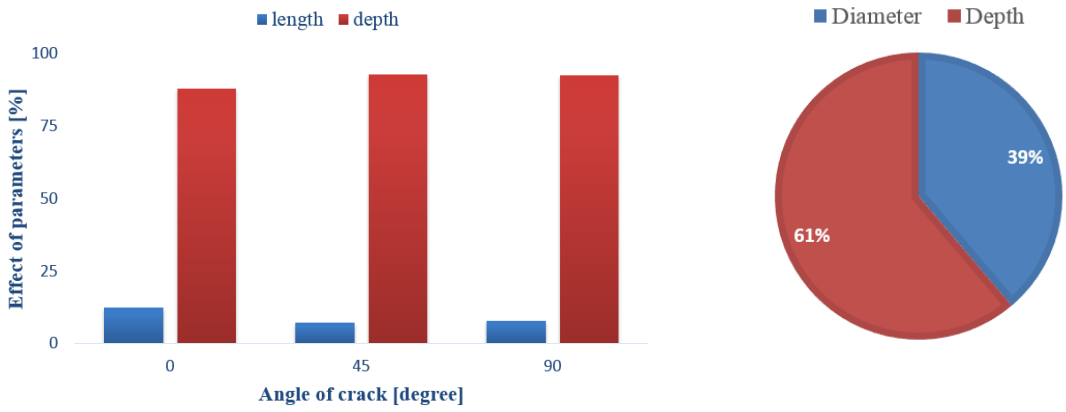

(**a**) (**b**)

Figure 11. (**a**) Effect of different parameters of the crack with various angles; (**b**) Impact of different parameters of the pitting corrosion defect in percentages.

6. Conclusions

It is shown that the most critical area for crack and pitting corrosion is the second region of the tank body, based on the software and analytical calculations, although in the first region with the highest thickness of the wall the hydrostatic pressure has a maximum value. However, the results show that the second region of the oil storage tank is critical because of its supporting conditions. Furthermore, the finite element results indicated that the most critical angle for the crack was 45 degrees. Moreover, the obtained results showed that the effect of the crack depth on the increase in stress was superior to the effect of the crack length. Additionally, for the defect of the pitting corrosion, the impact of the depth on the stress raising was superior to the impact of the diameter.

On the other hand, the progression towards the depth has a greater effect on the equivalent von Mises stress than the progression towards its length does. Moreover, the Taguchi analysis indicated that the effect of the crack depth on the maximum von Mises stress at the critical region of the oil storage tank was about 91% and that the effect of the crack length was 9%. In addition, the effects of the pit depth and diameter on the critical stress for the corrosion defect were about 61% and 39%, respectively.

Author Contributions: Conceptualization, M.O.B. and K.R.K.; methodology, M.O.B. and K.R.K.; software, M.O.B., K.R.K. and S.S.R.K.; validation, M.O.B., K.R.K. and S.S.R.K.; formal analysis, M.O.B., K.R.K. and S.S.R.K.; investigation, M.O.B., K.R.K., S.S.R.K. and M.P.; resources, S.S.R.K. and M.P.; data curation, M.O.B. and K.R.K.; writing—original draft, M.O.B. and K.R.K.; writing—review & editing, M.O.B., K.R.K. and S.S.R.K.; visualization, M.O.B., K.R.K., S.S.R.K. and M.P.; supervision, M.O.B., K.R.K. and S.S.R.K.; project administration, M.O.B., K.R.K., S.S.R.K. and M.P.; funding acquisition, S.S.R.K. and M.P. All authors have read and agreed to the published version of the manuscript.

Funding: The research was supported by the Ministry of Education, Youth, and Sports of the Czech Republic and the European Union (European Structural and Investment Funds Operational Program Research, Development, and Education) in the framework of the project "Modular platform for autonomous chassis of specialized electric vehicles for freight and equipment transportation", Reg. No. CZ.02.1.01/0.0/0.0/16_025/0007293, as well as the financial support from internal grants in the Institute for Nanomaterials, Advanced Technologies and Innovations (CXI), Technical University of Liberec (TUL).

Acknowledgments: The research was supported by the Ministry of Education, Youth, and Sports of the Czech Republic and the European Union (European Structural and Investment Funds Operational Program Research, Development, and Education) in the framework of the project "Modular platform for autonomous chassis of specialized electric vehicles for freight and equipment transportation", Reg. No. CZ.02.1.01/0.0/0.0/16_025/0007293, as well as the financial support from internal grants in the Institute for Nanomaterials, Advanced Technologies and Innovations (CXI), Technical University of Liberec (TUL).

Conflicts of Interest: The authors declare no conflict of interest.

References

1. Underwood, J. Stress Intensity Factors for Internally Pressurized Thick-Wall Cylinders. Stress analysis and growth of cracks. *ASTM STP* **1997**, *513*, 59–70.
2. Raju, I.S.; Newman, J. Stress-Intensity Factors for Internal and External Surface Cracks in Cylindrical Vessels. *Int. J. Press. Vessel. Technol.* **1982**, *104*, 293–298, doi:10.1115/1.3264220.
3. Carpinteri, A. Shape change of surface cracks in round bars under cyclic axial loading. *Int. J. Fatigue* **1993**, *15*, 21–26, doi:10.1016/0142-1123(93)90072-x.
4. Carpinteri, A.; Brighenti, R.; Spagnoli, A. Part-through cracks in pipes under cyclic bending. *Nucl. Eng. Des.* **1998**, *185*, 1–10, doi:10.1016/s0029-5493(98)00189-7.
5. Fonte, M.; De Freitas, M. Stress Intensity Factors for semi-elliptical surface cracks in round bars under bending and torsion. *Int. J. Fatigue* **1999**, *21*, 457–463, doi:10.1016/s0142-1123(98)00090-5.
6. De Fonte, M.; Gomes, E.; De Freitas, M. Stress Intensity Factors for Semi-Elliptical Surface Cracks in Round Bars Subjected to Mode I (Bending) and Mode III (Torsion) Loading. In *European Structural Integrity Society*; 1999; Vol. 25, pp. 249–260.
7. Bhuyan, G.S.; Sperling, E.J.; Shen, G.; Yin, H.; Rana, M.D. Prediction of Failure Behavior of a Welded Pressure Vessel Containing Flaws During a Hydrogen-Charged Burst Test. *J. Press. Vessel. Technol.* **1999**, *121*, 246–251, doi:10.1115/1.2883699.
8. Carpinteri, A.; Brighenti, R.; Spagnoli, A. Fatigue growth simulation of part-through flaws in thick-walled pipes under rotary bending. *Int. J. Fatigue* **2000**, *22*, 1–9, doi:10.1016/s0142-1123(99)00115-2.
9. Toughiry, M. Development of Accept Reject Criteria for Requalification of High Pressure Steel and Aluminium Cylinders. *STIN* **2002**, 3, 04229.
10. Shahani, A.R.; Habibi, S.E. Calculation of stress intensity factors for semi-elliptical surface cracks in thick-walled cylinders under bending moment—Part II: Numerical simulation. In Proceedings of the 14th Annual International Conference of Iranian Society of Mechanical Engineering, Isfahan, Iran, 15–17 May 2006.
11. Shahani, A.R.; Shoja, M.M.; Fazli, A.; Hosseinali, M. Calculation of stress intensity factors for semi-elliptical surface cracks in thick-walled cylinders under bending moment—Part I: Experimental observations. In

Proceedings of the 14th Annual International Conference of Iranian Society of Mechanical Engineering, Isfahan, Iran, 15-17 May 2006.

12. Wallbrink, C.; Peng, D.; Jones, R. Assessment of partly circumferential cracks in pipes. *Int. J. Fract.* **2005**, *133*, 167–181, doi:10.1007/s10704-005-0628-0.
13. Shahani, A.R.; Habibi, S.E. Stress Intensity Factors in a Hallow Cylinder Containing a Circumferential Semi-Elliptical Crack Subjected to Combined Loading. *Int. J. Fatigue* **2006**, *29*, 128–140.
14. Kaptan, A.; Kisioglu, Y. Determination of burst pressures and failure locations of vehicle LPG cylinders. *Int. J. Press. Vessel. Pip.* **2007**, *84*, 451–459, doi:10.1016/j.ijpvp.2007.02.004.
15. Kasai, N.; Fujiwara, Y.; Sekine, K.; Sakamoto, T. Evaluation of back-side flaws of the bottom plates of an oil-storage tank by the RFECT. *NDT E Int.* **2008**, *41*, 525–529, doi:10.1016/j.ndteint.2008.05.002.
16. Kim, J.-S.; An, D.-H.; Lee, S.-Y.; Lee, B. A failure analysis of fillet joint cracking in an oil storage tank. *J. Loss Prev. Process. Ind.* **2009**, *22*, 845–849, doi:10.1016/j.jlp.2009.08.014.
17. Godoy, L.A.; Batista-Abreu, J.C. Buckling of fixed-roof aboveground oil storage tanks under heat induced by an external fire. *Thin-Walled Struct.* **2012**, *52*, 90–101, doi:10.1016/j.tws.2011.12.005.
18. Yang, L.; Chen, Z.; Cao, G.; Yu, C.; Guo, W. An analytical formula for elastic–plastic instability of large oil storage tanks. *Int. J. Press. Vessel. Pip.* **2013**, *101*, 72–80, doi:10.1016/j.ijpvp.2012.10.006.
19. Kasai, N.; Mori, S.; Tamura, K.; Sekine, K.; Tsuchida, T.; Serizawa, Y. Predicting maximum depth of corrosion using extreme value analysis and Bayesian inference. *Int. J. Press. Vessel. Pip.* **2016**, *146*, 129–134, doi:10.1016/j.ijpvp.2016.08.002.
20. Cheng, X.; Jing, W.; Yin, C.; Li, C. Stability parameter analysis of a composite foundation of an oil storage tank in a loess area treated with compaction piles. *Soils Found.* **2018**, *58*, 306–318, doi:10.1016/j.sandf.2018.02.004.
21. Shigeno, H.; Okamoto, D.E.K. *Corrosion of Bottom Plate of Oil Storage Tank and Corrosion Control*; Nakagawa Corrosion Protecting Company, Ltd.: Tokyo, Japan, 1960.
22. Pence, A.W. *Failure Avoidance in Welded Fabrication*; National Board Bulletin, 1988, 17-23.
23. Kashyzadeh, K.R.; Farrahi, G.H.; Shariyat, M.; Ahmadian, M.T. Experimental and finite element studies on free vibration of automotive steering knuckle. *Int. J. Eng. (IJE) Trans. B Appl.* **2017**, *30*, 1776–1783.
24. Kashyzadeh, K.R. Effects of Axial and Multiaxial Variable Amplitude Loading Conditions on the Fatigue Life Assessment of Automotive Steering Knuckle. *J. Fail. Anal. Prev.* **2020**, *20*, 455–463, doi:10.1007/s11668-020-00841-w.
25. Kashyzadeh, K.R. A new algorithm for fatigue life assessment of automotive safety components on the probabilistic approach: The case study of steering knuckle. *Eng. Sci. Technol. Int. J.* **2020**, *23*, 392–4040.
26. Higdon, A.; Ohlsen, E.H.; Stiles, W.B.; Weese, J.A.; Riley, W.F. *Mechanics of Materials*, 4th ed.; John Wiley and Sons: Hoboken, NJ, USA, 1985.
27. *ABAQUS Analysis User Manual Version 6.6*; ABAQUS, Inc., Rising Sun Mills, 166 Valley Street, Providence, RI02909, USA, 2006.
28. *MSC/PATRAN & MSC/NASTRAN Analysis User Manual*; Universal Analytics Inc., Torrance, California USA, 2001.
29. Maleki, E.; Unal, O.; Kashyzadeh, K.R. Efficiency Analysis of Shot Peening Parameters on Variations of Hardness, Grain Size and Residual Stress via Taguchi Approach. *Met. Mater. Int.* **2019**, *25*, 1436–1447, doi:10.1007/s12540-019-00290-7.
30. Pandey, N.; Murugesan, K.; Thomas, H. Optimization of ground heat exchangers for space heating and cooling applications using Taguchi method and utility concept. *Appl. Energy* **2017**, *190*, 421–438, doi:10.1016/j.apenergy.2016.12.154.
31. Kashyzadeh, K.R.; Ghorbani, S.; Forouzanmehr, M. Effects of Drying Temperature and Aggregate Shape on the Concrete Compressive Strength: Experiments and Data Mining Techniques. *Int. J. Eng.* **2020**, *33*, 1780–1791, doi:10.5829/ije.2020.33.09c.12.
32. Zhao, L.; Zhao, Y.; Bao, C.; Hou, Q.; Yu, A. Optimization of a circularly vibrating screen based on DEM simulation and Taguchi orthogonal experimental design. *Powder Technol.* **2017**, *310*, 307–317.
33. Ghorbani, S.; Ghorbani, S.; Kashyzadeh, K.R. Taguchi approach and response surface analysis to design of a high-performance SWCNT bundle interconnects in a full adder. *Int. J. Eng. (IJE) Trans. B Appl.* **2020**, *33*, 1598–1607.

34. Chauhan, R.; Singh, T.; Kumar, N.; Patnaik, A.; Thakur, N. Experimental investigation and optimization of impinging jet solar thermal collector by Taguchi method. *Appl. Therm. Eng.* **2017**, *116*, 100–109, doi:10.1016/j.applthermaleng.2017.01.025.
35. Farrahi, G.; Kashyzadeh, K.R.; Minaei, M.; Sharifpour, A.; Riazi, S. Analysis of Resistance Spot Welding Process Parameters Effect on the Weld Quality of Three-steel Sheets Used in Automotive Industry: Experimental and Finite Element Simulation. *Int. J. Eng.* **2020**, *33*, 148–157, doi:10.5829/ije.2020.33.01a.17.